Peer-reviewed version available at Materials 2018, 11, 1005; doi:10.3390/ma11061005

Synergistic effect of graphene oxide and mesoporous structure on flame retardancy of nature rubber/IFR composites

Na Wang [1,2,*], Miao Zhang [1,2], Ping Kang[2], Jing Zhang[2], Qinghong Fang[2], Wenda Li[3]

[1] Sino-Spanish Advanced Materials Institute, Shenyang University of Chemical Technology, Shenyang 110142, China

[2] Liaoning Provincial Key Laboratory of Rubber & Elastomer, Shenyang 110142, China

[3] IMDEA Materials Institute, C/Eric Kandel 2, Getafe, 28906, Madrid, Spain

* Corresponding author: iamwangna@syuct.edu.cn. Tel.: 86-13840257976

Abstract: Aiming to improve the flame retardancy performance of natural rubber (NR), we developed a novel flame retardant synergistic agent through grafting of MCM-41 to graphene oxide (GO), named as GO-NH-MCM-41, as an assistant of intumescent flame retardants (IFR). The structure of GO-NH-MCM-41 was characterized by FTIR, TEM and SEM tests, which confirmed that a fine grafting had been applied between GO and MCM-41. The flame retardancy of NR/IFR/GO-NH-MCM-41 composites was evaluated by limited oxygen index (LOI), UL-94 and cone calorimeter test. The LOI value of NR/IFR/GO-NH-MCM-41 reached to 26.3%; the UL-94 ratings improved to V-0 rating. Moreover, the addition of GO-NH-MCM-41 obviously decreased the peak heat release rate (PHRR) and the total heat release (THR) of the natural rubber composites. And the addition of GO-NH-MCM-41 increased the thickness of char residue. The images of SEM indicated the char residue were more compact and continuous. The degradation of GO-NH-MCM-41 based NR composites completed with a mass loss of 35.57% at 600 ℃. The tensile strength and the elongation at break of NR/IFR/GO-NH-MCM-41 composites were 13.9 MPa and 496.7%, respectively. The results of rubber process analyzer (RPA) reached the maximum value, probably due to a better network of the fillers in the matrix.

Key words: natural rubber; GO-NH-MCM-41; graphene oxide; mesoporous; intumescent flame retardants

1. Introduction

Natural rubber is one of the most important thermoset polymers, widely used as economic industrial raw materials in various aspects due to its outstanding mechanical properties, chemical resistance and good insulation. Unfortunately, the high flammability of NR has hindered its wide applications [1-4]. Several methods were attempted to improve the flame retardancy of natural rubber. The IFR system is an effective way to improve the flame retardancy properties of NR; one of the widely used IFR systems consists of ammonium polyphosphate (APP), pentaerythritol (PER) and melamine (MEL) [5]. It has some advantages such as low smoke, less toxic, low loading and no melt dropping, etc. However, compared

Peer-reviewed version available at Materials 2018, 11, 1005; doi:10.3390/ma11061005

with halogen-containing flame retardants, IFR has some disadvantages on flame retardant efficiency and thermal stability, for example, IFR is easy to migrate to the composite surface. The polar groups in IFR molecules such as -OH and -NH_4 groups have poor compatibility with the non-polar polymer matrix, and thus led to a decrease in the flame retardancy and the thermal stability.

It is an effective approach to improve the flame retardancy and mechanical properties of flame retardancy natural rubber (FRNR) with the introduction of synergist flame retardant[6-9]. The application of graphene oxide as a synergist in NR system has become more and more popular. The graphene oxide can generate enormous insulating layers when the composite is heated, this is due to graphene oxide is composed of carbon atoms having two-dimensional crystal with only one atom layer. Due to its special tri-dimensional structure, it can increase the amount of char residue and improve the thermal stability of FRNR. The limiting oxygen index value increased with the addition of graphene oxide, and higher ratings were achieved in UL-94 test [10-12]. However, graphene oxide showed a tendency of aggrlomeration in the matrix, led to the recreation of pristine graphite due to the interactions of π electrons and Van der Waals forces [13,14].This resulted in inefficient dispersion of GO in polymer matrix, which has an negative influence on the mechanical properties of FRNR [15,16].

In our previous work, MCM-41 was used as a reinforced filler to enhance the mechanical and thermal properties of polymer materials[17,18]. Numerous publications have been devoted to the preparation, characterization and properties of polymer/mesoporous MCM-41 composites [19-22]. The NR/MCM-41 nanocomposite showed enhanced tensile modulus which was higher than that of neat NR [23]. MCM-41 and APP were used as the core of double-layered co-microencapsulation. MCM-41 provided many binding sites which strengthened the intumescent char [24]. We added GO-NH-MCM-41 as synergistic flame retardant into epoxy resin(EP), 2 wt% GO-NH-MCM-41 showed the exfoliated nano-dispersion in EP matrix, a 40.0% reduction of pHRR in cone calorimeter test was observed in EP/GO-NH-MCM-41 compared with EP/GO [25]. In this paper, the synergistic mechanism of GO-NH-MCM-41 in FRNR was investigated. The structure of GO-NH-MCM-41 was characterized by Fourier-transform infrared spectroscopy, transmission electron microscope and scanning electron microscopy. The effects of GO-NH-MCM-41 on flame retardancy properties of NR were measured by limiting oxygen index, UL-94 test, thermogravimetric analysis, cone calorimeter test and mechanical properties were characterized by tensile test and rubber process analyzer (RPA). The synergistic mechanism of GO and MCM-41 was also investigated.

2. Materials and Methods

2.1 Materials

The nano-sized mesoporous MCM-41 particle was prepared in our laboratory with a lateral size of 80–100 nm. The surface area and specific pore volume of the MCM-41 particles were 732 m^2/g and 0.9 cm^3/g; the lateral size of pore was only 3.6 nm. The nano-sized graphite was supplied by Beijing Deke Graphite Co., Ltd., China. Sulfuric acid (H_2SO_4, 98%), potassium permanganate ($KMnO_4$), hydrazine hydrate (85% aq), ammonia (25–28% aq), hydrogen peroxide (H_2O_2, 30% aq), hydrochloric acid (HCl, 37% aq, diluted to 5 wt% before

use) were used as received . NR SMR-20 was provided by Hainan state farms Group Co., Ltd. The commercial product APP (phase II, average degree of polymerization n > 1000, soluble in H_2O < 0.5 mass%) was supplied by Shifang Changfeng Chemical Co., Ltd., China. PER and MEL were supplied by Sinopharm Chemical Reagent Co., Ltd. The mass ratio of APP, PER, and MEL in IFR mixture was 3:1:1. Analytical grade zinc oxide (ZnO) was provided by Dalian zinc oxide factory. Accelerant CZ and tetramethylthiuram disulfide were purchased from Tianjin No.1 Organic Chemical Plant. Sulfur was purchased from Tong Chuang Chemical Co., Ltd., Taizhou. Carbon soot and age inhibitor 4010 were provided by Sheng Ao Chemical Co., Ltd., Shandong.

2.2 Methods

2.2.1 Preparation of GO

GO was obtained from natural graphite by modified Hummers method [26]. In brief, the graphite powder was treated with a solution containing a mixture of H_2SO_4, $K_2S_2O_8$ and P_2O_5 at 80°C to yield preoxidized graphite. Then, it was added into cold concentrated H_2SO_4 followed by $KMnO_4$ slowly. H_2O_2 and distilled water were used to terminate the reaction. The solution was filtered, washed with HCl solution and dried to obtain brown color solid. The obtained GO was exfoliated for about 30 min in water, in order to form stable GO dispersion (0.2 wt%).

2.2.2 Preparation of MCM-41–NH2

(3-aminopropyl)triethoxysilane (APTES) (1.024 mL) was used to modify MCM-41, the APTES solution was refluxed in toluene at 105°C for 120 min. This step was repeated three times to obtain MCM-41-NH_2 [27].

2.2.3 Preparation of GO-NH-MCM-41

Scheme for the synthesis of GO-NH-MCM-41 is shown in Fig. 1. Firstly, 1-ethyl-3-(3-dimethyl aminopropyl) carbodiimide (EDC) (0.035g) and N-hydroxysuccinimide (NHS) (0.023 g) were added into 20 ml distilled water. 11 mL of the above activiated solution were slowly added into 500 mL 0.2 wt% GO dispersion for about 2.5 h. Then MCM-41-NH_2 (5 g) was added into the above reaction mixture and stirred for 2 h at 40 °C. The resulting product GO-NH-MCM-41 was washed with distilled water and methanol for 2-3 times.

The GO-NH-MCM-41 was suspended in distilled water (400 mL) with strong stirring and ultrasonication at least for 1 h. Reduction was carried out at 80 °C in the presence of hydrazine hydrate (the weight of hydrazine hydrate was as same as GO). Stirring and ultrasonication should be carried throughout the whole preparation process. The GO-NH-MCM-41 powder was isolated via filtration, and washed with distilled water for four times, then dried to remove residual solvents at 60 °C for 24 h.

Preprints (www.preprints.org) | NOT PEER-REVIEWED | Posted: 9 May 2018 doi:10.20944/preprints201805.0138.v1

Peer-reviewed version available at Materials 2018, 11, 1005; doi:10.3390/ma11061005

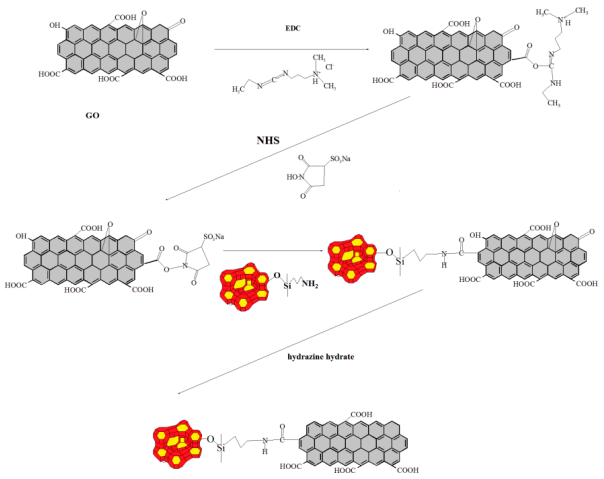

Fig. 1 Reaction process of GO-NH-MCM-41

2.2.4 Preparation of FRNR composites

FRNR composites were synthesized by different proportions of IFR agents with NR by two-roll mill. The compositions of FRNR composites are listed in Table. 1. The fixed values of NR components like carbon soot, stearic acid, zinc oxide, sulfur, age inhibitor 4010, electric insulating oil, accelerant CZ, and tetramethylthiuram disulfide were 35, 5, 5, 4, 1.2, 1, 1, 0.8 and 0.35 phr respectively. All NR composites were vulcanized at 145°C at certain pressure for the optimum cure time t90, determined by a GT-M2000-A rheometer (GaoTie Limited Co., Taiwan). Then all specimens were cut into vulcanized sheets at 20°C for 24 h before test.

Table. 1 Ingredients of NR composites

Samples	**NR/phr**	**IFR/phr**	**MCM-41/phr**	**GO/phr**	**GO-MCM-41/phr**
NR	100				
NR/IFR	100	40			
NR/IFR/MCM-41	100	39	1		
NR/IFR/GO	100	39		1	
NR/IFR/GO-MCM-41	100	39			1

2.2.5 Characterization

The fourier transform infrared spectra of samples were measured with a Nicolet MNGNA-IR 560 with 4 cm^{-1} resolution. Limiting oxygen index (LOI) data were obtained by an oxygen index instrument (JF-3) (Jiangning Analysis Instrument Co., China) according to GB/T 10707-2008 standard. The dimensions of the specimens were 126 mm×6.5 mm×3 mm

and all the composites were tested for five times. The vertical burning tests (UL-94 test) were carried out on a CZF-3 type instrument (Jiangning Analysis Instrument Co., China) according to GB/T 10707-2008 standard. The dimensions of the specimens were 130 mm×13 mm×3 mm. Room-temperature tensile tests of the composites were conducted on an Instron 1211 testing machine, according to GB/T528-1998 standard, at a crosshead speed of 500 mm/min. The cone calorimeter tests were carried out on a Fire Testing Technology (FTT, UK) cone calorimeter. The square specimens (100mm×100 mm×4 mm) were irradiated at a heat flux of 35 kW/m^2 according to ISO 5660 standard procedures without the use of "frame and grid" and the exhaust flow was set at 24 L/s. Each sample was tested twice. The Scanning electron microscopy (SEM) images of NR composites were obtained with a scanning electron microscope JEOL JSM-6360LV. The specimens were previously coated with a conductive gold layer. The burnt samples from LOI were used for testing. Complete burning of samples was ensured. Thermal stability of NR composites was examined on a Perkin-Elmer TGA 7 thermal analyzer. The heating rate was set at 10 °C/min, and approximately 10 mg of samples were tested under nitrogen with a flow rate of 90 mL/min from room temperature to 700°C. Curing was performed on rubber process analyzer RPA-8000 (GaoTie Limited Co., Taiwan) at 145°C with a frequency of 100 cpm, and strain amplitude of 0.5°. For strain sweep, the temperature was set to 60°C; the frequency was set to 60 cpm, and the strain was between 1% and 100%.

3. results and discussion

3.1 Characterization of GO-NH-MCM-41

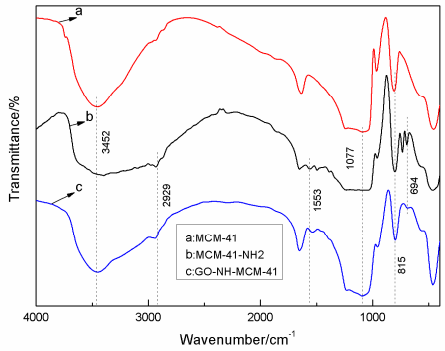

Fig. 2 FTIR spectra of flame retardant synergist

FTIR spectra of samples are shown in Fig. 2. The absorption bands at 3452 cm^{-1} indicated the presence of surface silanols and adsorbed water molecules. The absorption peaks at 1077 cm^{-1} and 815 cm^{-1} were due to the asymmetric stretching vibrations of Si-O-Si bridges. MCM-41-NH_2 showed visible absorption peaks at 2929 cm^{-1} and 1553 cm^{-1}, corresponding to CH_2 stretching and bending vibration of -NH- groups, respectively (Fig. 2b), proved the successful amine functionalization. After grafting GO to MCM-41-NH_2, the intensity of -NH- stretching, -NH- bending, and Si-O stretching vibrations decreased in FTIR spectrum (Fig. 2c), because the -H atoms attached to amine group were consumed by grafting MCM-41-NH_2 with GO. It indicated that GO-NH-MCM-41 was successfully achieved by grafting[28].

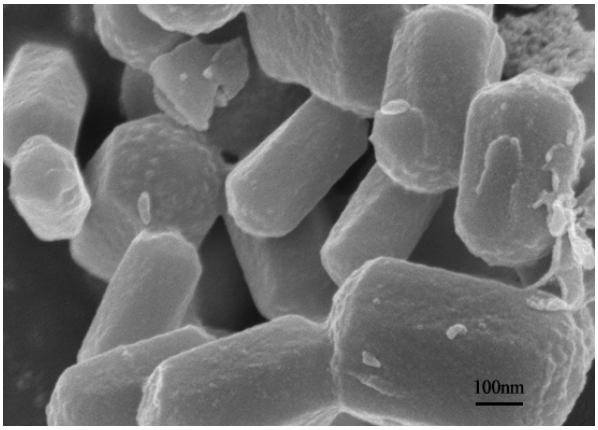

Fig. 3 SEM images of GO-NH-MCM-41

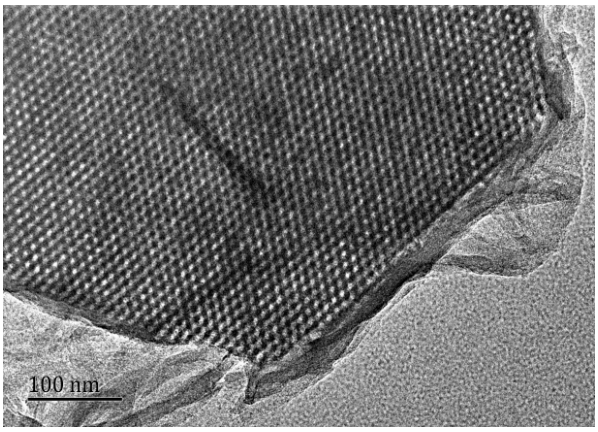

Fig. 4 TEM image of GO-NH-MCM-41

Fig. 3 and Fig. 4 showed the SEM and TEM images of GO-NH-MCM-41. As shown in Fig. 3, the surface of MCM-41 coated with GO was not flat; it indicated that a fine coating of GO was formed by the poly-condensation reaction of GO. Fig. 4 showed the TEM images of the calcined GO-NH-MCM-41 sample. It can be noticed that the mesopores formed with highly ordered hexagonal array surrounded by graphene sheets. From the image, it was notable that MCM-41 had a good compatibility with GO, which is consistent to the analysis of the FTIR spectrum. According to the above analysis, the flame retardant synergist GO-NH-MCM-41 was synthesized by grafting.

3.2 Flame retardancy

Table. 2 Flame retardancy and mechanical properties of FRNR composites

Samples	**LOI/%**	**UL-94**	**Tensile strength/MPa**	**Elongation at break/%**
NR	18.2	No rating	18.9	581.3
NR/IFR	22.4	V-1	9.5	479.6

NR/IFR/MCM-41	25.6	V-0	11.6	485.8
NR/IFR/GO	24.3	V-1	11.5	493.7
NR/IFR/GO-NH-MCM-41	26.3	V-0	13.9	496.7

The flame retardancy properties and mechanical properties of composites were tested using standard tests. The data of the UL-94 ratings and LOI tests are summarized in Table. 2. The LOI value of pure NR was only 18.2%, showing high flammability. When the traditional IFR was added into NR, the LOI value of NR/IFR composite was increased to 22.4% and with no rating in UL-94 test. Meanwhile, when MCM-41 was used as the synergistic agent, the LOI values of NR/IFR/MCM-41 composites reached to 25.6% and achieved V-0 rating in UL-94 test. It can be explained that the addition of MCM-41 can reduce the amount of amorphous char in order to protect and strengthen the intumescent char [29]. When GO was used as synergistic agent, the LOI value of NR/IFR/GO composite reached to 24.3% and achieved V-1 rating in UL-94 test. This phenomenon was probably explained that the presence of GO could facilitate the formation of strong char layers which could delay weight loss caused by the decomposition [30]. In addition, the LOI value of FRNR composite containing GO-NH-MCM-41 was 26.3%, showed an obvious increase by 17.4% compared to NR/IFR systems. The three-dimensional structure and binding sites of GO-NH-MCM-41 contributed to the ability of catalytic char layers. It also increased the oxidative degradation temperature and decreased the oxidization heat. It confirmed that GO-NH-MCM-41 can act as an excellent flame retardant synergist in improving the fire safety properties of NR.

3.3 Mechanical properties

The mechanical properties of NR and FRNR composites are shown in Table. 2. The tensile strength and elongation at break of NR were 18.9 MPa and 591.3%, whereas 9.5 MPa and 479.6% for NR/IFR composites, respectively. It was found that the addition of traditional IFR can remarkably decrease the mechanical properties of NR composites. The great difference in polarity between NR matrix and IFR fillers led to the incompatibility and bad dispersion [31]. In contrast, when MCM-41 and GO were used as flame retardant synergistic agents separately, the tensile strength and elongation at break increased. Due to the large specific surface area and massive binding sites of MCM-41 and GO, the polar groups present in synergist, such as amine and hydroxy group, can form hydrogen bonds with the amine groups of intumescent flame retardant. It dispersed well and formed a better interaction with rubber matrix than IFR [32]. The maximum values of tensile strength and elongation at break of GO-NH-MCM-41 reached to 13.9 MPa and 496.7%, higher than the values of MCM-41 and GO. This result confirmed that the GO-NH-MCM-41 can improve not only the flame retardancy properties but also the mechanical properties.

3.4 Cone calorimetry

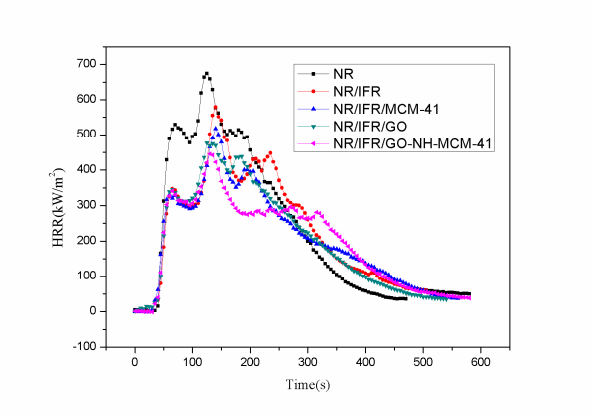

Fig. 5 HRR curves of NR and FRNR composites

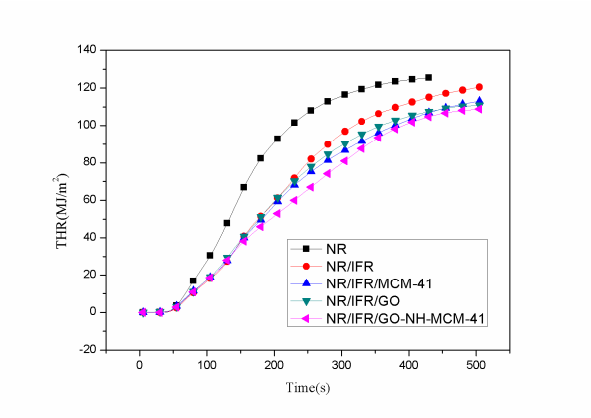

Fig. 6 THR curves of NR and FRNR composites

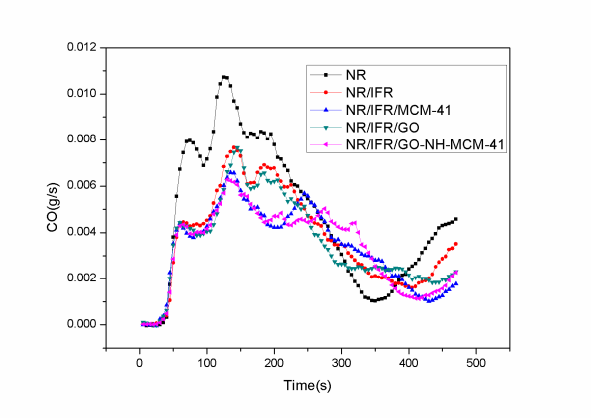

Fig. 7 CO curves of NR and FRNR composites

Preprints (www.preprints.org) | NOT PEER-REVIEWED | Posted: 9 May 2018 doi:10.20944/preprints201805.0138.v1

Peer-reviewed version available at Materials 2018, 11, 1005; doi:10.3390/ma11061005

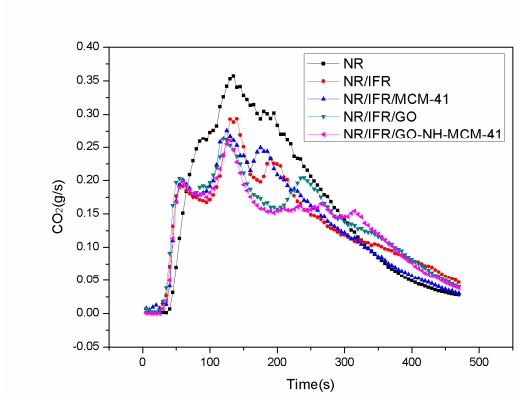

Fig. 8 CO_2 curves of NR and FRNR composites

Table. 3 Cone data of FRNR composites

Samples	PHRR(kW/m²)	THR(MJ/m²)	P-CO(g/s)	P-CO_2(g/s)
NR	675	128	0.0107	0.3567
NR/IFR	518	115	0.0077	0.2936
NR/IFR/MCM-41	477	113	0.0076	0.2759
NR/IFR/GO	455	124	0.0066	0.2636
NR/IFR/GO-MCM-41	446	109	0.0063	0.2601

Cone calorimetry is considered as the most effective characterization to investigate the flammability behavior of materials in real fire scenarios due to its good correlation with real fire disasters [33]. The images and data of cone calorimeter test are shown in Fig. 4, Fig. 5, Fig. 6, Fig. 7 and Table. 3, respectively. In Fig. 5, the HHR curves of NR and IFR were double-peak pattern [34]. Because the rubber component was heated, its surface was cross-linked and carbonized, the carbon layers blocked oxygen and heat from outside. At this time the combustion behavior was suppressed and the first peak appeared, but as the combustion depth increased, the surface carbon layers were destroyed, the rubber under the carbon layers continued to crack, releasing more combustible gas, THR and HRR reached the maximum peak value. So we can easily kown that the burning of natural rubber was intense, its flame retardancy was low. When IFR was added into NR, this situation was changed in a manner, the values of PHRR and THR decreased by 23.3% and 10.5%. This phenomenon was due to the flame retardancy of IFR. The char layers were formed by IFR, which can block the exchange of oxygen and heat from inside and outside. The degree of combustion was controlled, but the char layers were not firm enough. So we tried to find a way to increase the strength of the carbon layer on the base of not reducing the mechanical properties. When

Preprints (www.preprints.org) | NOT PEER-REVIEWED | Posted: 9 May 2018 doi:10.20944/preprints201805.0138.v1

Peer-reviewed version available at Materials 2018, 11, 1005; doi:10.3390/ma11061005

MCM-41 and GO were used as synergistic agents, PHRR values decreased to 477 kW/m^2 and 455 kW/m^2, respectively. As discussed before, it may due to the strong ability of MCM-41 and GO to enhance char layers. These results revealed that flame retardancy properties of NR can be improved by the addition of synergistic agents MCM-41 and GO. And PHRR of NR/IFR/GO-NH-MCM-41 composites showed an obvious decrease by 34% compared to NR system, which was lower than other samples. Particularly, THR, CO yield and CO_2 yield of NR/IFR/GO-NH-MCM-41 composites decreased by 14%, 50% and 39% respectively, compared to NR. The notable reduction in fire hazard was mainly attributed to the synergistic effect between physical barrier and catalytic effect of GO and MCM-41. when the surface carbon layers of NR/IFR/GO-NH-MCM-41 were destroyed, the internal rubber will form a new carbon layer so repeated, and there will be a stationary combustion period. The carbon layers can improve the barrier ability of the carbon layer in the future combustion period, Thus, with the synergistic effect of IFR, it could promote the formation of intumescent char layers and these layers can efficiently prevent the transfer of heat and gas between flame zone and burning substrate.

3.5 Thermal stability

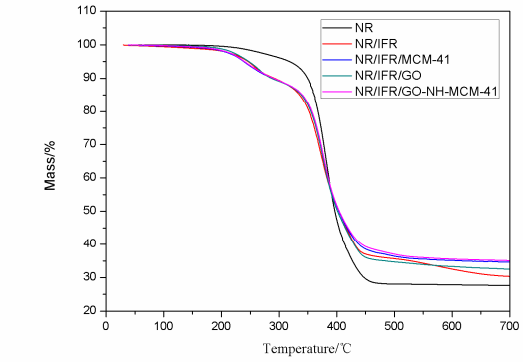

Fig. 9 TG curves of NR and FRNR composites

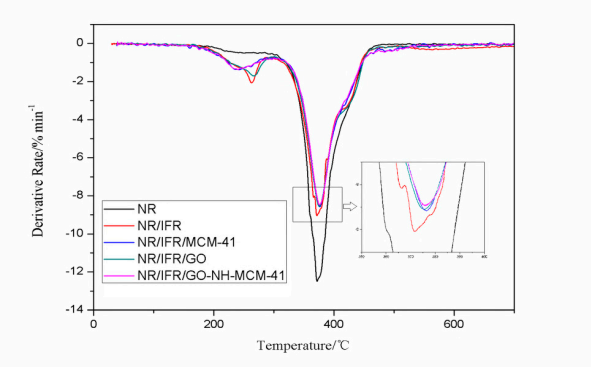

Fig. 10 DTG curves of NR and FRNR composites

Table. 4 TG data of FRNR composites

Flame retardant composites	T10%/℃	T20%/℃	T50%/℃	W600/%
NR	349.92	367.35	396.72	27.86
NR/IFR	292.17	352.07	403.76	32.54
NR/IFR/MCM-41	289.74	356.85	403.71	35.12
NR/IFR/GO	287.32	354.98	401.39	33.32
NR/IFR/GO-MCM-41	290.76	356.78	404.59	35.57

TG was used to characterize the thermal degradation of composites. The related data of TG are listed in table. 4. The 10wt% weight loss temperature of NR/IFR was decreased to 292℃, approximately 16% reduce compared to that of pure NR, because IFR had poor thermal stability, and could decompose at 200℃ before the degradation temperature of NR matrix, PER produced ester polyols and the acid as dehydrating agent, ester polyols carbonized that produced molecular of water to decrease the temperature of environment, the acid had the esterification reaction with PER to form a carbon layers. MEL and APP also produced uncombustible gas NH_3 which expanded the carbon layers. At the beginning of combustion, the char layers were too thin to prevent oxygen and heat to diffuse into the matrix. As the surface area of combustion boundary increased, the combustion process developed more quickly. After the initial degradation, the intumescent char layers generated, and the diffusion rate of volatile combustible fragments by thermal degradation slowed down, and the mass loss rate decreased. The degradation of NR/IFR/GO-NH-MCM-41 ended with a mass loss of 35.57%, higher than other samples. It was found that FRNR composites achieved better thermal stability in presence of the intumescent flame retardants. Because it could decompose into polyphosphoric acid, water gas and ammonia gas at high temperature. They might get coated at the surface of matrix to prevent the heat from diffusing into matrix, so that temperature gradient between char layers and matrix was increased. It may suggest that the enhancement in char residue was due to the heat resistance of GO-NH-MCM-41. GO had an excellent thermal property and expanded several hundred times along C-C axial when it was heated. The residue of NR/IFR/GO-NH-MCM-41 was more continuous and compact than others, so the protective barrier had an excellent property to limit the transfer of flammable molecules to gas phase.

3.6 Morphologies of burnt composites

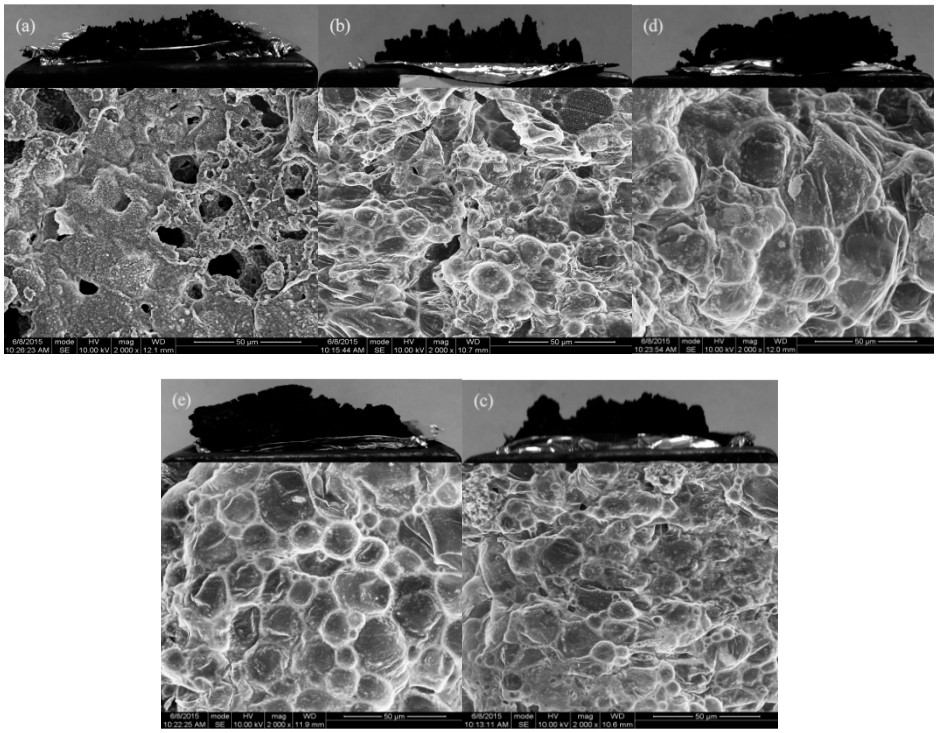

Fig. 11 Morphology of burnt composites (a) NR (b) NR/IFR (c) NR/IFR/MCM-41 (d) NR/IFR/GO (e) NR/IFR/GO-NH-MCM-41

It was known that a continuous and compact char layer can act as an insulating barrier to heat. Meanwhile, it can also prevent the access of oxygen during combustion. In order to investigate the char layer morphology of burnt NR composites, the samples were collected from LOI test. The SEM images are shown in Fig. 11. As shown in Fig. 11a, there were a number of deep cavities and holes on the surface of NR mixture after the combustion. Relatively loose structure including cracks and cavities appeared on the surface of char residues. In NR/IFR systems, some hollows could be seen in fractured char(Fig. 11b). When MCM-41 and GO were used as synergistic agent, the char layer of NR systems (Fig. 11c and Fig. 11d) became more compact with fewer holes, compared to that of NR/IFR systems. However, we can hardly find holes on the surface of char layers in NR/IFR/GO-NH-MCM-41 (Fig. 11e). More continuous and compact char layer structure was obtained for the NR composites. In addition, more uniform blisters can also be observed in the image. This indicated that GO-NH-MCM-41 was effective in forming more compact char layers, because GO-NH-MCM-41 had good compatibility with matrix and formed network structure at high temperature in fire hazard situation.

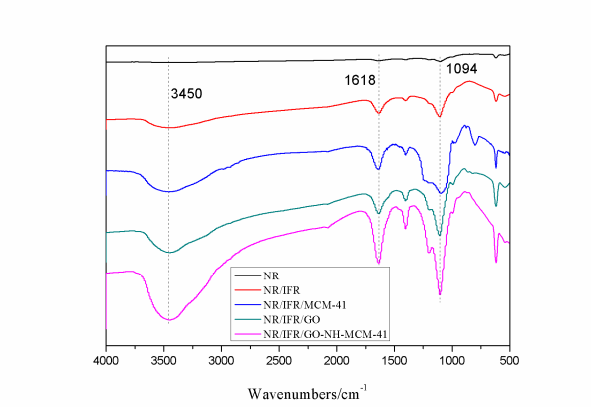

Fig. 12 FTIR spectra of char residues of FRNR composites after burning

To investigate the structure and compositions of char residues, FTIR spectra of char residues was recorded and shown in Fig. 12. These char residues were obtained by heating the samples in a muffle furnace at 600℃ for 10 min. The absorption peak at 3450 cm^{-1} was attributed to water molecule. The absorption peak at 1618 cm^{-1} revealed the presence of multi-aromatic structure in the char residue. NR composites showed the similar char structure due to similar spectrum of pure NR. An intensive absorption peak at 1094 cm^{-1} was assigned to vibrations of P-O-C group. It was found that stretching vibration intensity of different chemical groups increased from top to bottom, which proved the increase in flame retardancy products. The char layers, composed of multi-aromatic carbon and phosphorus-containing structures, exhibited high thermal stability, and thus acted as an effective barrier to protect the matrix from decomposition at high temperature.

3.7 RPA

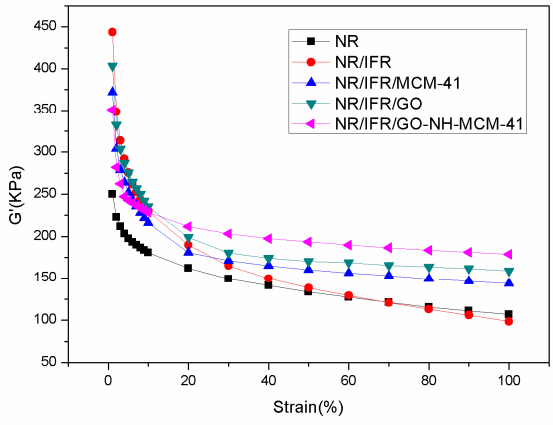

Fig. 13 Dependence of G' on strain of NR and FRNR composites

Table. 5 ΔG' values

Sample	$\Delta G'$/MPa
NR	1.18
NR/IFR	3.45
NR/IFR/MCM-41	2.28
NR/IFR/GO	2.45
NR/IFR/GO-MCM-41	1.72

The dependence of G' on strain of NR and FRNR composites are shown in Fig. 13 and Table. 5. The filler network was broken down due to the application of small strain, this was generally called Payne effect [35]. ΔG' was often used as an indicator for the strength of filler network. Because G' value decreased as the filler network strength reduced. It can be clearly seen from Fig. 13 that all composites showed a typical Payne effect. In addition, the G' values of all composites decreased at 1% strain. At the same time, while increasing the strain, the values of G' decreased gradually. The G' almost reached the stable value as the unfilled rubber arrived the ultimate strain of 100%. From Table. 5, it can be obviously seen that the ΔG' values of composites decreased in the following order: NR/IFR > NR/IFR/GO > NR/IFR/MCM-41 > NR/IFR/GO-NH-MCM-41. Therefore, the strength of the filler network increased in the order of NR/IFR/GO-NH-MCM-41 > NR/IFR/MCM-41 > NR/IFR/GO > NR/IFR. This was because GO-NH-MCM-41 had an optimized compatibility with matrix. As a result, NR/IFR/GO-NH-MCM-41 had the strongest filler network among FRNR composites, and thus GO-NH-MCM-41 had a positive effect in improving the mechanical properties of natural rubber composites.

4. Conclusions

In conclusion, GO-NH-MCM-41 had outstanding flame retardancy properties. It increased the LOI values of FRNR composites from 22.4% to 26.3% and achieved V-0 rating in UL-94 test. The PHRR, THR, CO yield and CO2 yield of NR/IFR/GO-NH-MCM-41 composites decreased by 34%, 14%, 50% and 39% respectively. The char layers of NR/IFR/GO-NH-MCM-41composites were more compact and continuous. GO-NH-MCM-41 as synergist improved thermal stability of NR through increasing the char residue which could delay weight loss and reduce the risk of fire hazard. It was mainly attributed to the synergistic effect between physical barrier and catalytic property of GO-NH-MCM-41.

The good mechanical properties of NR/IFR/GO-NH-MCM-41 composite were attributed to high specific surface area and the presence of large number of pores in GO-NH-MCM-41. The fine grafting between GO and MCM-41 resulted in a better dispersion and filler network in composites. The values of tensile strength and elongation at break of NR/IFR/GO-NH-MCM-41 were higher than NR/IFR/MCM-41 and NR/IFR/GO.

Acknowledgements: The authors gratefully acknowledge the financial support of the Finance Refers to Top Talents of Liaoning Province (Grant Nos.[2016]864), the BaiQianWan Talents Program of Liaoning Province (Grant Nos.[2017]62), Innovative Talents Program of Universities in Liaoning Province (Grant Nos.[2017]053), Science and Technology Program of Shenyang (Grant No: 17-51-6-00), Shenyang Scientific and Technological Innovation Talents Program for Youngs and Middles(Grant No: RC170118) and Shenyang science and technology bureau, Sino-Spanish Advanced Materials Institute(Grant No:18-005-6-04).

References

1. Larissa NC, Cássio RR, Aline Z, Raquel S M, Marcelo G, Rosmary NB, Janaina S C. Characterization of natural rubber nanocomposites filled with organoclay as a substitute for silica obtained by the conventional two-roll mill method. Appl Clay Sci. 2011;52:56–61.
2. Huang GB, Li YJ, Han L, Gao JR, Wang X. A novel intumescent flame retardant-functionalized montmorillonite: preparation, characterization, and flammability properties. Applied Clay Science. 2011; 51: 360–5.
3. Sharma R, Sharma N. A thermal behaviour and structural study of bis(hydroxamato)oxovanadium(IV) complexes. J Therm Anal Calorim. 2013; 112: 25–30.
4. Chandrasekar S, Sarathi R, Danikas MG. Analysis of surface degradation of silicone rubber insulation due to tracking under different voltage profiles. Electri Eng. 2007; 89: 489–501.
5. Sebastian R, Yuttapong C, Bernhard S. Exploring the Modes of Action of Phosphorus-Based Flame Retardants in Polymeric Systems. Mater. 2017; 10: 445-68.
6. Iqbal SS, Inam F, Iqbal N, Jamil T, Bashir A, Shahid M. Ther-mogravimetric, differential scanning calorimetric, and experimental thermal transport study of functionalized nanokaolinitedoped elastomeric nanocomposites. J Therm Anal Calorim. 2016; 125(2): 871–80.
7. Federico C, Jenny A, Chiara P, and Alberto F. Improving the Flame Retardant Efficiency of Layer by Layer Coatings Containing Deoxyribonucleic Acid by Post-Diffusion of Hydrotalcite Nanoparticles. Mater. 2017; 10; 709-21.
8. Andrea T, Péter N, Ákos P, György M, Beáta S. Flame Retardancy of Carbon Fibre Reinforced Sorbitol Based Bioepoxy Composites with Phosphorus-Containing Additives. Mater. 2017; 10: 467-79.
9. Zhang X, Alloul O, Zhu J, He Q, Luo Z, Colorado HA, Haldolaarachchige N, Young DP, Shen T, Wei S. Iron-core carbon-shell nanoparticles reinforced electrically conductive magnetic epoxy resin nanocomposites with reduced flammability. RSC Adv. 2013; 3: 9453–64.
10. Mohammad R, Babak S, Chil-Hung C. Study of Adsorption Mechanism of Congo Red on Graphene Oxide/PAMAM Nanocomposite. Mater. 2018; 11: 496-520.
11. Bai H, Li C, Shi GQ. Functional composite materials based on chemically converted graphene. Adv Mater. 2011; 23: 1089–115.
12. Bao CL, Song L, Xing WY, Yuan BH, Wilkie CA, Huang JL, Guo YQ, Hu Y. Preparation of graphene by pressurized oxidation and multiplexreduction and its polymer nanocomposites by masterbatch-based melt blending. J Mater Chem. 2012; 22:6088–96.
13. Wang X, Song L, Yang HY, Xing WY, Lu HD, Hu Y. Simultaneous reduction and surface functionalization of graphene oxide with POSS for reducing fire hazards in epoxy composites. J Mater Chem. 2012; 22: 22037–43.
14. Zhong JQ, Liang S, Xiong QY, et al. Approximate microwave heating models for global temperature profile in rectangular medium with TE_{10} mode. J Therm Anal Calorim. 2015; 122: 487–95.
15. Chen HD , Wang JH, Ni AQ, Ding AX, Han X, Sun ZH. The Effects of a Macromolecular Charring Agent with Gas Phase and Condense Phase Synergistic Flame Retardant Capability on the Properties of PP/IFR Composites. Mater. 2018; 11; 111-26.
16. Sengupta R, Bhattacharya M, Bandyopadhyay S, Bhowmick AK. A review on the mechanical and electrical properties of graphite and modified graphite reinforced polymer composites. Prog Polym Sci. 2011; 36: 638–70.

17. Wang N, Shao ZX, Zhang J, Zhang HW. Preparation and characterization of epoxy composites filled with functionalized nano-sized MCM-41 particles. J Mater Sci. 2008; 43: 3683–8.
18. Wang N, Fang QH, Chen EF, Zhang J. Preparation and characterization of polypropylene composites filled with different structured mesoporous particles. Compos sci. 2010; 42: 2083–93.
19. Wang N, Gao N, Fang QH, Chen EF. Compatibilizing effect of mesoporous fillers on the mechanical properties and morphology of polypropylene and polystyrene blend. Mater Des. 2011; 32: 1222–8.
20. Wang N, Wu YX, Zhang J, Ma Chi, Chen EF. Compatibilizing effect of MCM-41 and PP-g-MAH on the mechanical and thermal analyzer of PP/PS blends. Adv Mater Res. 2012; 391: 278–81.
21. Wang N, Fang QH, Zhang J, Chen EF, Zhang XB. Incorporation of nano-sized mesoporous MCM-41 material used as fillers in natural rubber composite. Mater Sci Eng A. 2011; 528: 3321–25.
22. Wang N, Zhang J, Fang QH, David Hui. Influence of mesoporous fillers with PP-g-MA on flammability and tensile behavior of polypropylene composites. Compos Part B. 2013; 44: 467–471.
23. Wang N, Gao N, Jiang S, Fang QH, Chen EF. Effect of different structure MCM-41 fillers with PP-g-MA on mechanical properties of PP composites. Composites . 2011; 42: 1571–7.
24. Wang N, Xu G, Wu YH, Zhang J, Hu LD ,Luan HH, Fang QH. Double-layered co-microencapsulated ammonium polyphosphate and mesoporous MCM-41 in intumescent flame-retardant natural rubber composites. J Therm Anal Calorim. 2016; 123; 1239–51.
25. Li Z, Alejandro JG, Vignesh BH, Wang DY. Covalent assembly of MCM-41 nanospheres on graphene oxide forimproving fire retardancy and mechanical property of epoxy resin. Compos Part B.2018; 138; 101-112.
26. William S Hummers Jr, Richard E Offeman. Preparation of graphitic oxide. J Am Chem Soc, 1958;80: 1339.
27. Rostamizadeh S, Azad M, Shadjou N, Hasanzadeh M. (α-Fe_2O_3)-MCM-41-SO_3H as a novel magnetic nanocatalyst for the synthesis of N-aryl-2-amino-1,6-naphthyridine derivatives. Catal Commun. 2012; 25: 83–91.
28. Wang N, Mi L, Wu Y. Double-layered co-microencapsulated ammonium polyphosphate and mesoporous MCM-41 in intumescent flame-retardant natural rubber composites. J Therm Anal Calorim. 2014; 115: 1173–81.
29. Huang T, Lu RG. Chemically modified graphene/polyimide composite films based on utilization of covalent bonding and oriented distribution. Appl Mater Interf. 2012; 4: 2699–708.
30. Janowska G, Kucharska-Jastrząbek A, Rybiński P, Wesołek D, Wójcik I. Flammability of diene rubbers. J Therm Anal Calorim. 2010;102:1043–49.
31. Sophie W, Thiebault C, Martin B, Khalifah AS, Sabyasachi G. Recent Developments in Organophosphorus Flame Retardants Containing P-C Bond and Their Applications. Mater. 2017; 10; 784-816.
32. Maciejewska M. Thermal properties of TRIM–GMA copolymers with pendant amine groups. J Therm Anal Calorim. 2016; 126: 1777–85.
33. Sun HQ, Liu SZ, Wang SB. Reduced graphene oxide for catalytic oxidation of aqueous organic pollutants. Appl Mater Interfaces. 2012;4: 5466–5471.
34. Chen CC, Li Z, Shi L, et al. Thermoelectric Transport Across Graphene/Hexagonal Boron Nitride/Graphene Heterostructures. Nano Research, 2015,8(2): 666–672.
35. Robertson CG, Lin CJ, Bogoslovov RB, Rackaitis M, Sadhukhan P, Quinn JD, Roland CM. Reinforcement, and glass transition effects in silica-filled styrene-butadiene rubber. Rubber Chem Technol. 2011;84:507–19.